

Synthesis, Biological Activity, Molecular Modelling Studies and 3D-QSAR Investigations of *N*-[2-(aryl/substituted aryl)-4-oxo-1, 3-thiazolidin-3-yl]pyridine-4-carboxamides

Asha B. Thomas^{a,*}, Rabindra K. Nanda^a, Lata P. Kothapalli^a, Piyush A. Sharma^b and Kishori G. Apte^c

^aDepartment of Pharmaceutical Chemistry, Padm. Dr. D.Y. Patil Institute of Pharmaceutical Sciences and Research, Pune, Maharashtra, India

^bDepartment of Pharmaceutical Chemistry, Sri Aurobindo Institute of Pharmacy, Indore, Madhya Pradesh, India

^cNational Toxicology Centre (NTC), Pune, Maharashtra, India

Abstract: In the present research work new 4-thiazolidinones possessing dual cyclooxygenase/lipoxygenase inhibition were synthesized. Sixteen *N*-[2-(aryl/substitutedaryl)-4-oxo-1,3-thiazolidin-3-yl]pyridine-4-carboxamide derivatives (5a-q) differing by the phenyl group substitution were synthesized by sonication. Compounds *N*-[2-(4-chlorophenyl)-4-oxo-1, 3-thiazolidin-3-yl] pyridine-4-carboxamide (5d) and *N*-[2-(4-nitrophenyl)-4-oxo-1, 3-thiazolidin-3-yl] pyridine-4-carboxamide (5f) showed promising anti-inflammatory activity investigated by the carrageenan induced edema model in rats. Compound 5f, was the most active in the series with low ulcerogenic index and good safety profile with highest *in vitro* inhibition of COX-1/COX-2 (89.28; 52.80%, $p < 0.01$) with 27.36% inhibition of 15-LOX. Compounds 5d and 5f, at the dose of 100mg/kg p.o. were also effective in lowering the elevated levels of AST, ALT and ALP in serum and also lowered the elevated levels of MPO in edematous tissue comparable to standard anti-inflammatory drug, Indomethacin. The Autodock investigation of the synthesized compounds within the COX and LOX enzymes predicted fairly good correlation between the anti-inflammatory activities (IC_{50}) and their binding affinities. The 3D-QSAR studies (V-Life Molecular Design Software) of the synthesized 4-thiazolidinones for their anti-inflammatory activity by the developed kNN, PLRS and MLR models suggested that presence of electron withdrawing functional groups like $-NO_2$, $-Cl$ on the phenyl ring were favourable for activity. The results of the present study may help to identify the relative positions and ranges of important electrostatic and steric fields at various positions around the pharmacophore that could be useful in the design of new molecules with improved anti-inflammatory activity.

Keywords: Anti-inflammatory activity, 3D-QSAR, dual COX/LOX inhibitors, microwave irradiation, Schiff's bases, sonication, 4-thiazolidinones.

INTRODUCTION

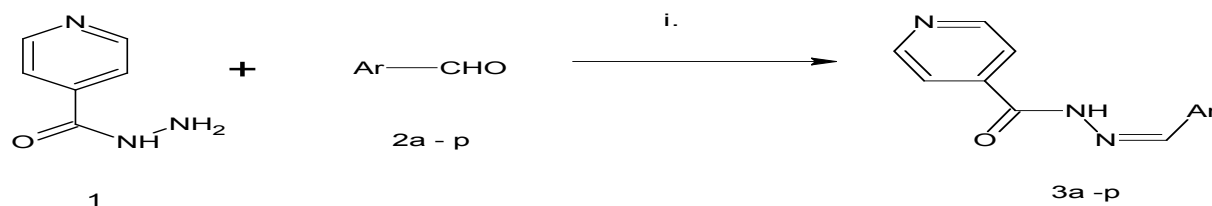
Non-steroidal anti-inflammatory drugs are of huge therapeutic benefit in the treatment of rheumatoid arthritis and various types of inflammatory conditions by blocking the production of prostanoids from arachidonic acid through inhibition of cyclooxygenase (COX) activity. Recent evidence also suggests that anti-inflammatory drugs could be beneficial in a number of neurodegenerative disorders including Alzheimer's and Parkinson's diseases, which have a prominent neuroinflammatory component [1, 2]. However their long term clinical use is associated with significant side effects such as gastric ulcers, gastrointestinal lesions, bleeding and nephrotoxicity which limit their clinical applications [3]. Therefore, there is a constant need for development of novel drugs with better safety profiles that could be used long term to relieve various chronic

inflammatory conditions. Besides COXs, 5-lipoxygenase (LOX) is an important metabolic enzyme for formation of leukotrienes from arachidonic acid (AA), leading to inflammation and other pathological responses. Combined with the earlier studies that COX inhibition alone may lead to an up regulation of AA metabolism by the 5-LOX pathway, it is now appreciated that dual inhibition against both COXs and 5-LOX might present an enhanced anti-inflammatory potency without risk of serious side effects including gastric damage. Thus, a single agent inhibiting both enzymes has been of interest to medicinal chemists.

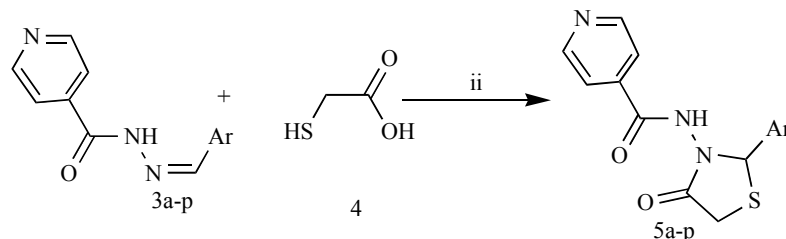
In recent year's computational chemistry, especially quantitative structure-activity relationship (QSAR) studies have become an integral part of the drug discovery process [4]. The 3D-QSAR predictions allow medicinal chemists to identify three dimensional pharmacophores which are essential and important for biological activity resulting in successful lead development [5].

Of particular importance are the 4-thiazolidinones because of their varied biological properties [6]. Many 4-Thiazolidinone analogues show anticonvulsant [7, 8], antibacterial [9-11], antifungal [12, 13], ischemic [14], anti-

*Address correspondence to this author at the Department of Pharmaceutical Chemistry, Padm. Dr. D.Y. Patil Institute of Pharmaceutical Sciences and Research, Pimpri, Pune-411018, MH India; Tel: +91-9881236220; Fax No.: +91-020-27420261; E-mail: dypharmachem@yahoo.co.in



Scheme (1). Microwave assisted synthesis of intermediate Schiff's bases of INH,



Scheme (2). Synthesis of 4-thiazolidinone analogues using Schiff's bases.

HIV [15] and anticancer activities [16]. In recent years, research has focused on the study of 4-thiazolidinones as anti-inflammatory and analgesic agents [17-20]. However there are no reports on the QSAR studies of 4-thiazolidinones for their anti-inflammatory activity.

Diarylheterocycles, and other central ring pharmacophore templates, have been extensively studied as cyclooxygenase inhibitors. All these tricyclic molecules possess 1, 2-diaryl substitution on a central four-, five- or six-membered ring system. Several derivatives containing pyrazoline, thiophene, di-tert-butylphenol, hydrazone, pyrrolidine and pyrazole subunits have been found to be dual COX/LOX inhibitors. A number of reported dual COX/LOX inhibitors like Licoflone are nitrogen containing heterocycles [21].

Based of the above findings and considering the need to identify new candidates that may be of value in designing new, potent and less toxic anti-inflammatory agents, we report herein in the present work the synthesis and anti-inflammatory screening of some 4-thiazolidinone derivatives starting from isonicotinic acid hydrazide by the green route method of sonication, their anti-inflammatory screening, molecular docking and 3D-QSAR studies.

EXPERIMENTAL SECTION

All research chemicals were purchased from Acros organics (NY, USA), Sigma-Aldrich (St. Louis, Missouri, USA) and used as such for the reactions. Melting points (mp) were determined on a Veego melting point apparatus (VMP PM, 32/1104) and are uncorrected. Reactions were monitored by thin layer chromatography carried out using pre-coated silica gel plates (E. Merck and Co., Darmstadt, Germany). UV studies were carried out on a UV Visible spectrophotometer (Shimadzu 1700). The IR spectra (KBr) were recorded on a FTIR spectrophotometer with Diffuse Reflectance attachment (Shimadzu 8400S). ¹H NMR spectra were obtained on a NMR Spectrophotometer (Bruker Avance II 400 NMR) using dimethyl sulphoxide-d₆ as the solvent. The mass spectra were obtained on a Hewlett Packard Electron Impact mass spectrometer GCD-1800A (70 eV EI source) using direct insertion probe and Quadrupole TOF Mass spectrometer using electrospray ionisation

(Positive mode). Microanalyses were performed on a Thermo Finnigan C, H, N analyzer.

Synthesis

N'-(1*Z*)-(aryl/substituted aryl)methylidene]pyridine-4-carboxamides(3a-p)

According to our previously reported procedure, the Schiff's bases (3a-p) were synthesized (Scheme 1). The compounds were characterised on the basis of spectral and analytical data (UV, IR, ¹H NMR, MS, CHN) [22, 23].

Reagents and conditions: i. H₂O, MWI, Power level 3(240 W, 35% irradiation)

N-[2-(aryl/substitutedaryl)-4-oxo-1, 3-thiazolidin-3-yl] pyridine-4-carboxamides(5a-p)

The synthesized Schiff's bases (3a-p) were converted to their 4-thiazolidinones (5a-p) as per our reported green route method of sonication (Scheme 2) and characterized by their analytical and spectral data [24].

Reagents and conditions: ii. Anhydrous ZnCl₂, molecular sieves [MS (1-2 gms, 3A X 1.5 mm)], THF, sonication.

***N*-(4-oxo-2-phenyl-1,3-thiazolidin-3-yl)pyridine-4-carboxamide(5a).** White powder, yield 92.0%, mp 250-253^oC, IR (ν_{max}, cm⁻¹, KBr): 3256 (-NH), 3028 (-CH), 1743 (ring -C=O), 1650 (amide-I C=O). ¹H NMR (400 MHz, DMSO-d₆): δ ppm 8.77,8.68 (d, Pyridine 2H); 8.75 (s, NH 1H); 7.75,7.73 (d, Pyridine 2H); 7.51(s, Aromatic 5H); 5.96 (s, CH 1H); 3.40, 3.36 (d, CH₂ 1H); 3.27,3.23 (d, CH₂ 1H). MS: m/z 299(M)⁺. Anal. Calcd for C₁₅H₁₃N₃O₂S (299.35): C, 60.18; H, 4.38; N, 14.04%. Found: C, 59.82; H, 4.42; N, 14.22%.

***N*-[2-(2-hydroxyphenyl)-4-oxo-1,3-thiazolidin-3-yl]pyridine-4-carboxamide(5b).** White powder, yield 89.7%, mp 268-271^oC, IR (ν_{max}, cm⁻¹, KBr): 3344 (-OH), 3217 (-NH), 3039 (-CH), 1739 (ring -C=O), 1697 (amide I,C=O). ¹H NMR (400 MHz, DMSO-d₆): δ ppm 9.04,8.98 (d, Pyridine 2H); 8.12,8.11 (d, Pyridine 2H); 7.54 (s, NH 1H);7.47-6.87 (m, Aromatic 4H); 6.22 (s, OH 1H); 5.69 (s, CH 1H); 3.48, 3.44 (d, CH₂ 1H); 3.29,3.25 (d, CH₂ 1H). MS: m/z 316.6(M + H)⁺. Anal. Calcd for C₁₅H₁₃N₃O₃S (315.35): C, 57.13; H, 4.16; N, 13.33%. Found: C, 57.27; H, 4.12; N, 13.19%.

N-[2-(4-hydroxyphenyl)-4-oxo-1,3-thiazolidin-3-yl]pyridine-4-carboxamide(5c). Yellow powder, yield 90.2%, mp >290°C, IR (ν_{\max} , cm^{-1} , KBr): 3445 (-OH), 3217 (-NH), 3052 (-CH), 1724 (ring C=O), 1668 (amide I, C=O). ^1H NMR (400 MHz, DMSO- d_6): δ ppm 8.77, 8.75 (d, Pyridine 2H); 8.06 (s, NH 1H); 7.85, 7.84 (d, Pyridine 2H); 7.75, 7.73 (d, Aromatic 2H); 7.34, 7.29 (d, Aromatic 2H); 6.05 (s, CH 1H); 5.36 (s, OH 1H); 3.70, 3.66 (d, CH₂ 1H); 3.59, 3.54 (d, CH₂ 1H). MS: m/z 315(M)⁺. Anal. Calcd for C₁₅H₁₃N₃O₃S (315.35): C, 57.13; H, 4.16; N, 13.33%. Found: C, 57.38; H, 3.92; N, 13.66%.

N-[2-(4-chlorophenyl)-4-oxo-1,3-thiazolidin-3-yl]pyridine-4-carboxamide(5d). White crystals, yield 96.8%, mp 239-242°C, IR (ν_{\max} , cm^{-1} , KBr): 3159 (-NH), 3082 (-CH), 1728 (ring C=O), 1674 (amide I, C=O), 1083 (-C-Cl). ^1H NMR (400 MHz, DMSO- d_6): δ ppm 8.77, 8.75 (d, Pyridine 2H); 8.07 (s, NH 1H); 7.85, 7.84 (d, Pyridine 2H); 7.75, 7.73 (d, Aromatic 2H); 7.71, 7.69 (d, Aromatic 2H); 6.05 (s, CH 1H); 3.70, 3.77 (d, CH₂ 1H); 3.60, 3.64 (d, CH₂ 1H). MS: m/z 333(M)⁺. Anal. Calcd for C₁₅H₁₂ClN₃O₂S (333.79): C, 53.97; H, 3.62; N, 12.59%. Found: C, 55.02; H, 3.89; N, 12.02%.

N-[2-(3-chlorophenyl)-4-oxo-1,3-thiazolidin-3-yl]pyridine-4-carboxamide(5e). White crystals, yield 89.2%, mp 215-218°C, IR (ν_{\max} , cm^{-1} , KBr): 3070 (-NH), 3024 (-CH), 1708 (ring C=O), 1693 (amide I, C=O), 1076 (-C-Cl). ^1H NMR (400 MHz, DMSO- d_6): δ ppm 8.92, 8.91 (d, Pyridine 2H); 8.33 (s, NH 1H); 8.16, 8.14 (d, Pyridine 2H); 7.60 (s, Aromatic 1H); 7.88 -7.56 (m, Aromatic 3H), 5.48 (s, CH 1H); 3.46, 3.42 (d, CH₂ 1H); 3.22, 3.18 (d, CH₂ 1H). MS: m/z 334.9(M + H)⁺. Anal. Calcd for C₁₅H₁₂ClN₃O₂S (333.79): C, 53.97; H, 3.62; N, 12.59%. Found: C, 54.31; H, 3.55; N, 12.42%.

N-[2-(4-nitrophenyl)-4-oxo-1,3-thiazolidin-3-yl]pyridine-4-carboxamide(5f). Yellow powder, yield 86.4%, mp 263-266°C, IR (ν_{\max} , cm^{-1} , KBr): 3120 (-NH), 3060 (-CH), 1720 (ring C=O), 1681 (amide I, C=O), 1519, 1338 (-NO₂). ^1H NMR (400 MHz, DMSO- d_6): δ ppm 9.07, 9.02 (d, Pyridine 2H); 8.73 (s, NH 1H); 8.13, 8.11 (d, Pyridine 2H); 7.95, 7.93 (d, Aromatic 2H); 7.71, 7.70 (d, Aromatic 2H); 5.91 (s, CH 1H); 3.39, 3.35 (d, CH₂ 1H); 3.30, 3.26 (d, CH₂ 1H). MS: m/z 344(M)⁺. Anal. Calcd for C₁₅H₁₂N₄O₄S (344.35): C, 52.32; H, 3.51; N, 16.27%. Found: C, 52.58; H, 3.68; N, 16.43%.

N-[2-(3-nitrophenyl)-4-oxo-1,3-thiazolidin-3-yl]pyridine-4-carboxamide(5g). Brown powder, yield 82.4%, mp 249-252, IR (ν_{\max} , cm^{-1} , KBr): 3159 (-NH), 3082 (-CH), 1728 (ring C=O), 1674 (amide I, C=O), 1523, 1350 (-NO₂). ^1H NMR (400 MHz, DMSO- d_6): δ ppm 8.92, 8.90 (d, Pyridine 2H); 8.33 (s, NH 1H); 8.16, 8.14 (d, Pyridine 2H); 7.88-7.86 (m, Aromatic 2H); 7.60-7.56 (m, Aromatic 2H); 5.48 (s, CH 1H); 3.46, 3.42 (d, CH₂ 1H); 3.22, 3.18 (d, CH₂ 1H). MS: m/z 345.6(M + H)⁺. Anal. Calcd for C₁₅H₁₂N₄O₄S (344.35): C, 52.32; H, 3.51; N, 16.27%. Found: C, 52.44; H, 3.59; N, 16.16%.

N-[2-(2-nitrophenyl)-4-oxo-1,3-thiazolidin-3-yl]pyridine-4-carboxamide(5h). Yellow powder, yield 82.9%, mp 255-258°C, IR (ν_{\max} , cm^{-1} , KBr): 3180 (-NH), 3066 (-CH), 1712 (ring C=O), 1666 (amide I, C=O), 1523, 1350 (-NO₂). ^1H NMR (400 MHz, DMSO- d_6): δ ppm 9.02, 8.81 (d, Pyridine 2H); 8.73 (s, NH 1H); 8.27, 8.25 (d, Aromatic 1H); 8.07, 8.05 (d, Pyridine 2H); 7.96-7.57 (m, Aromatic 3H); 6.38

(s, CH 1H); 3.79, 3.75 (d, CH₂ 1H); 3.26, 3.22 (d, CH₂ 1H). MS: m/z 344.5(M + H)⁺. Anal. Calcd for C₁₅H₁₂N₄O₄S (344.35): C, 52.32; H, 3.51; N, 16.27%. Found: C, 52.41; H, 3.59; N, 16.33%.

N-[2-(4-fluorophenyl)-4-oxo-1,3-thiazolidin-3-yl]pyridine-4-carboxamide(5i). Yellow powder, yield 94.2%, mp 240-242°C, IR (ν_{\max} , cm^{-1} , KBr): 3147 (-NH), 3082 (-CH), 1731 (ring C=O), 1666 (amide I, C=O), 1222 (-C-F). ^1H NMR (400 MHz, DMSO- d_6): δ ppm 8.89, 8.88 (d, Pyridine 2H); 8.03, 7.98 (d, Pyridine 2H); 7.66 (s, NH 1H); 7.45, 7.44 (d, Aromatic 2H); 7.06, 7.05 (d, Aromatic 2H); 5.33 (s, CH 1H), 3.41, 3.37 (d, CH₂ 1H); 3.18, 3.14 (d, CH₂ 1H). MS: m/z 318.5(M + H)⁺. Anal. Calcd for C₁₅H₁₂FN₃O₃S (317.34): C, 56.77; H, 3.81; N, 13.24%. Found: C, 56.82; H, 3.87; N, 13.61%.

N-[2-(4-methoxyphenyl)-4-oxo-1,3-thiazolidin-3-yl]pyridine-4-carboxamide(5j). Brown powder, yield 90.3%, mp 278-281°C, IR (ν_{\max} , cm^{-1} , KBr): 3267 (-NH), 3040 (-CH), 1710 (ring C=O), 1658 (amide I, C=O), 1448 (-CH₃). ^1H NMR (400 MHz, DMSO- d_6): δ ppm 8.75, 8.74 (d, Pyridine 2H); 8.42 (s, NH 1H); 7.83, 7.85 (d, Pyridine 2H); 7.74, 7.72 (d, Aromatic 2H); 6.95, 6.93 (d, Aromatic 2H); 5.89 (s, CH 1H); 3.86, 3.82 (d, CH₂ 1H); 3.76, 3.75 (d, CH₂ 1H), 3.59 (s, -OCH₃ 3H). MS: m/z 330.6(M + H)⁺. Anal. Calcd for C₁₆H₁₅N₃O₃S (329.37): C, 58.34; H, 4.59; N, 12.76%. Found: C, 58.58; H, 4.63; N, 12.80%.

N-{4-oxo-2-[(E)-2-phenylethenyl]-1,3-thiazolidin-3-yl}pyridine-4-carboxamide(5k). Yellow powder, yield 87.2%, mp 247-250°C, IR (ν_{\max} , cm^{-1} , KBr): 3148 (-NH), 3010 (-CH), 1718 (ring C=O), 1660 (amide I, C=O), 1622 (-C=C), 1421 (-CH). ^1H NMR (400 MHz, DMSO- d_6): δ ppm 8.76, 8.75 (d, Pyridine 2H); 8.27 (s, NH 1H); 7.85, 7.84 (d, Pyridine 2H); 7.52-7.30 (m, Aromatic 5H); 7.02, 6.98 (d, alkene 2H); 5.43 (s, CH 1H); 3.71, 3.69 (d, CH₂ 1H); 3.68, 3.65 (d, CH₂ 1H). MS: m/z 342.6(M + H)⁺. Anal. Calcd for C₁₈H₁₉N₃O₃S (341.43): C, 63.32; H, 5.61; N, 12.31%. Found: C, 63.49; H, 5.65; N, 12.33%.

N-[2-(4-hydroxy-3-methoxyphenyl)-4-oxo-1,3-thiazolidin-3-yl]pyridine-4-carboxamide(5l). Pale yellow powder, yield 80.3%, mp 217-219°C, IR (ν_{\max} , cm^{-1} , KBr): 3400 (-OH), 3149 (-NH), 3008 (-CH), 1710 (ring C=O), 1658 (amide I, C=O), 1392 (-OH). ^1H NMR (400 MHz, DMSO- d_6): δ ppm 7.85, 7.84 (d, Pyridine 2H); 8.75, 8.74 (d, Pyridine 2H); 8.38 (s, NH 1H); 7.42 (s, -OH 1H); 7.08-6.86 (m, Aromatic 3H); 5.85 (s, CH 1H); 3.91 (s, -OCH₃ 3H); 3.68, 3.66 (d, CH₂ 1H); 3.56, 3.54 (d, CH₂ 1H). MS: m/z 346.5(M + H)⁺. Anal. Calcd for C₁₆H₁₅N₃O₄S (345.37): C, 55.64; H, 4.38; N, 12.17%. Found: C, 55.79; H, 4.47; N, 12.20%.

N-(2-furan-2-yl-4-oxo-1,3-thiazolidin-3-yl)pyridine-4-carboxamide(5m). Brown powder, yield 81.0%, mp 198-201°C, IR (ν_{\max} , cm^{-1} , KBr): 3271 (-NH), 3112 (Furan ring -CH), 3066 (-CH-), 1714 (ring C=O), 1664 (amide I, C=O), 1542, 1404 (Furan ring C=C). ^1H NMR (400 MHz, DMSO- d_6): δ ppm 9.71, 9.70 (d, Pyridine 2H); 8.11 (s, NH 1H); 7.83, 7.80 (d, Pyridine 2H); 7.45-6.41 (m, Furfural ring 3H); 5.99 (s, CH 1H); 3.94, 3.90 (d, CH₂ 1H); 3.66, 3.62 (d, CH₂ 1H). MS: m/z 290.4(M + H)⁺. Anal. Calcd for C₁₃H₁₁N₃O₃S (289.31): C, 53.97; H, 3.83; N, 14.52%. Found: C, 54.12; H, 3.88; N, 14.61%.

N-[2-[4-(dimethylamino)phenyl]-4-oxo-1,3-thiazolidin-3-yl]pyridine-4-carboxamide(5n). Brown powder, yield 81.6%, mp 224-226^oC, IR (ν_{\max} , cm⁻¹, KBr): 3434 (-NH), 3190 (-CH), 1720 (ring C=O), 1664 (amide I, C=O), 1367 (-CH₃). ¹H NMR (400 MHz, DMSO-d₆): δ ppm 8.76, 8.75 (d, Pyridine 2H); 8.34 (s, NH 1H); 7.86, 7.85 (d, Pyridine 2H); 7.71, 7.69 (d, Aromatic 2H); 6.71, 6.68 (d, Aromatic 2H); 5.22 (s, CH 1H); 3.93, 3.91 (d, CH₂ 1H); 3.85, 3.84 (d, CH₂ 1H); 3.10 (s, -OCH₃ 3H); MS: m/z 343.6 (M + H)⁺. Anal. Calcd for C₁₇H₁₈N₄O₂S (342.42): C, 59.63; H, 5.30; N, 16.36%. Found: C, 59.78; H, 5.41; N, 16.44%.

N-[2-(5-nitrothiophen-2-yl)-4-oxo-1,3-thiazolidin-3-yl]pyridine-4-carboxamide(5o). Blackish brown powder, yield 94.3%, mp 174-176^oC, IR (ν_{\max} , cm⁻¹, KBr): 3120 (-NH), 3082 (thiophene -CH), 1712 (ring C=O), 1672 (amide I, C=O), 1500, 1336 (-NO₂). ¹H NMR (400 MHz, DMSO-d₆): δ ppm 8.78, 8.77 (d, Pyridine 2H); 7.97 (s, NH 1H); 7.86, 7.85 (d, Pyridine 2H); 7.44, 7.43 (d, Thiophene 2H); 5.69 (s, CH 1H); 3.53, 3.54 (d, CH₂ 1H); 3.45, 3.46 (d, CH₂ 1H). MS: m/z 351.5 (M + H)⁺. Anal. Calcd for C₁₃H₁₀N₄O₄S₂ (350.37): C, 44.56; H, 2.88; N, 15.99%. Found: C, 44.70; H, 2.95; N, 16.04%.

N-[2-(3-hydroxynaphthalen-2-yl)-4-oxo-1,3-thiazolidin-3-yl]pyridine-4-carboxamide(5p). Brown powder, yield 93.9%, mp 258-260^oC, IR (ν_{\max} , cm⁻¹, KBr): 3300 (-OH), 3200 (-NH), 3076 (-CH), 1716 (ring C=O), 1650 (amide I, C=O), 1458 (-OH). ¹H NMR (400 MHz, DMSO-d₆): δ ppm 10.85 (s, OH); 6.9, 8.67 (d, Pyridine 2H); 7.96 (s, NH 1H); 8.05, 8.03 (d, Pyridine 2H); 7.84-7.82 (m, Aromatic 2H); 7.63-7.59 (m, Aromatic 3H); 7.44-7.40 (m, Aromatic 1H); 5.95 (s, CH 1H); 3.53, 3.54 (d, CH₂ 1H); 3.48, 3.47 (d, CH₂ 1H). MS: m/z 366.6 (M + H)⁺. Anal. Calcd for C₁₉H₁₅N₃O₃S (365.41): C, 62.45; H, 4.14; N, 11.50%. Found: C, 62.58; H, 4.18; N, 11.60%.

Biological Investigations

Experimental Animals

Swiss albino mice of either sex (20-30 g) were used for the biological studies. They were housed under standard laboratory conditions, maintained on a natural dark and light cycle and had free access to food and water. Animals were acclimatized to laboratory conditions before the experimentation. The screening protocol was approved by the Institutional Ethics Committee and conducted according to the Indian National Science Academy Guidelines for the use and care of experimental animals (Protocol Nos.: DYPIPSR/586-25/2010; RP.No.048).

Acute Toxicity Study

The acute toxicity study for test 4-thiazolidinones were carried out in mice according to OECD guidelines [25]. Different doses of test drugs were administered at graded doses up to 2000 mg/kg, p.o. and animals were monitored individually and continuously for a period of up to 14 days for behavioral changes, toxic reactions and mortality.

Evaluation of Anti-Inflammatory Activity

Carrageenan Induced Paw Edema Inhibition Model in Rats

The study was performed by the procedure of Winter *et al.* [26]. Albino rats received a subplanter injection of 0.05

ml saline containing 1% carrageenan in the right hind paw of each rat. A suspension of tested compounds (graded doses of 25, 50, 100 and 200 mg/kg p.o.), standard drug Indomethacin (10 mg/kg, p.o.), or an equivalent volume of vehicle (gum acacia 2%) were administered intraperitoneally 1 hr before carrageenan injection. Control animals received the same volume of vehicle. The paw volume was measured by plethysmometry (UGO Basile 7140) immediately after the injection. Subsequent readings of the volume of the same paw were carried out at 60 min intervals and compared to the initial readings.

Measurement of Serum Levels of Marker Enzymes (AST, ALT and ALP)

The biochemical changes were investigated at the end of the 5 hrs study; the animals were sacrificed under light ether anaesthesia. Blood samples were collected by cardiac puncture and serum was separated by centrifugation at 2500 rpm below 30^oC for 30 min. The levels of marker enzymes; aspartate transaminase (AST), alanine transaminase (ALT) and alkaline phosphatase (ALP) were determined using biochemical kits [27, 28].

Myeloperoxidase Levels in Edematous Tissue in the Carrageenan Induced Paw Edema Model

Myeloperoxidase (MPO) activity, an indicator of polymorphonuclear leukocyte accumulation was determined following the procedure of Mullane *et al.* [29, 30]. After 5 hrs following injection of carrageenan, the hind paw edematous tissues were obtained and weighed. Each piece of tissue was homogenised in a solution containing 0.5% (w/v) hexadecyltrimethyl-ammonium bromide dissolved in 10mM potassium phosphate buffer (pH 7) and centrifuged for 30 min at 20,000 g at 4^oC. An aliquot of the supernatant was then allowed to react with a solution of ortho-dianisidine dihydrochloride (1.6mM) and 0.1mM hydrogen peroxide. The rate of change in absorbance was measured spectrophotometrically at 650 nm. Optical density units were converted into units of concentration using the molar absorptivity coefficient for the oxidized form of o-dianisidine [$\epsilon = 10,062 \text{ X (M X cm)}^{-1}$]. MPO activity was defined as the quantity of enzyme degrading 1 μmol of peroxide/min at 37^oC and expressed in U/100 mg of wet tissue.

Ulcerogenic Study in Mice

Acute ulcerogenic effect was investigated as described by Barf *et al.* in the same animals that were submitted to the anti-inflammatory evaluation. Briefly, animals were euthanized at the end of the experiments and the stomachs were excised along its greater curvature for visualization of gastric lesions with a stereomicroscope [31].

Assessment of COX Inhibitory Activity (COX-1/2 Assay)

The COX-1/2 inhibitory activities of the test thiazolidinones were measured using ovine COX-1/2 enzymes included in the COX inhibitory screening assay kit provided by Cayman (Item No.760111; Cayman Chemical Co., MI). The inhibitor screening assay is based on the measurement of the peroxidase component of COXs assayed colorimetrically by monitoring the appearance of oxidized N,N,N',N'-tetramethyl-p-phenylenediamine (TMPD) at 590 nm [32]. The inhibitory activity were tested at an arachidonic

acid substrate concentration of 1 μM and 0.1 μM respectively for COX-1/2 assay. The test compounds and standard Indomethacin were added to the reaction mixture at a concentration of 200 μM .

Assessment of Soybean Lipoxygenase Inhibitory Activity

The Lipoxygenase (LOs) inhibitory activity was assessed using the Cayman's Lipoxygenase Inhibitor Screening Assay Kit (Item No.:760700) which detects and measures the hydroperoxides produced in the lipoxygenation reaction and is a general detection method for LO, and can be used to screen libraries of compounds which inhibit LO enzymes [33].

Molecular Docking Study

The advanced docking program AutoDock 4.2 was used to evaluate the binding free energy of the inhibitors within the macromolecules and to gain insight into the binding modes of active 4-thiazolidinones.

Selection and Preparation of Ligands and Target Protein Crystal Structures

The ligands (4-thiazolidinones) were studied for their binding activities into COX-1/2 and 15-LOX enzymes. The three dimensional structures of the aforementioned compounds were drawn in PRODRG server using JME Molecular Editor; then energy minimization was performed with the ffgmx GROMACS force field by steepest descent for at most 50,000 steps, extended by 11 additional atom types to accommodate halogens, sp-hybridized atoms and other chemical features. The crystal structure of COX-1 in complex with Ibuprofen (1EQG; resolution- 2.61 \AA), COX-2 in complex with SC-558(1CX2; resolution-3.0 \AA) and LOX (1LOX; resolution-2.4 \AA) was extracted from the RCSB Protein Data Bank [34]. All bound water molecules, hetero atoms and ligands were removed from the proteins and polar hydrogens were added. For the targets, the amino acids of the ligand binding sites were defined using data in pdbsum [35].

Grid Generation and Run of Molecular Docking

The grid maps representing the native ligands in the actual docking target sites were calculated with AutoGrid. The grids were chosen to be sufficiently large to include not only the active site but also significant portions of the surrounding surface. The three dimensional grids, 60 \AA grid size (x, y, z) with a spacing of 0.375 \AA , were created. The cubic grid box was centered in the active region and encompassed the binding site where the ligands were embedded. Of the three different search algorithms offered by AutoDock, the GA-LS search algorithm (Genetic algorithm with local search) was chosen to search for the best conformers [36]. The parameters were set using ADT (Autodock Tool Kit) on PC associated with Autodock 4.2. For all docking parameters, default values were used with 50 independent docking runs for each docking case.

Molecular Docking and Analysis of the Docked Results

In the molecular docking studies, both the binding free energy and docking energy generated by Autodock was employed as the criterion for ranking. Cluster analysis was performed on the docked results using a root mean square

(RMS) tolerance of 0.5. Each of the clusters that exhibited significant negative interaction energies was examined by Accelrys, Discovery Studio Visualizer v2.0. [Accelrys Inc., San Diego, CA (2007)] to determine their binding orientations, molecular modeling, evaluation of the hydrogen bonds and for measuring RMSD, which was measured as distance between the centroids of the docked inhibitor and the native ligand. The mode of interaction of the native ligand within enzymes was used as the standard docked model as well as for RMSD calculation. The correct hydrogen bond interaction was considered according to Spoel *et al.* [37].

3D-QSAR Studies

The 3D-QSAR analysis of the synthesized N-[2-(aryl/substituted aryl)-4-oxo-1, 3-thiazolidin-3-yl]pyridine-4-carboxamide derivatives(5a-p) for their anti-inflammatory activity was performed using VLife MDS (Version 3.5, V Life Sciences) [38].

Biological Data

Data sets of 4-Thiazolidinones with sufficient range of anti-inflammatory activity were used for the present 3D-QSAR investigations. The biological activity (IC_{50} , mM) were converted to logarithmic values and subsequently used as dependent variables for the QSAR analysis.

Energy Minimization and Alignment of Molecules

All compounds were built on workspace of molecular modelling software VLife MDS 3.5. The structures were then converted to three-dimensional space for further analysis. All molecules were batch optimized for minimization of energies using Merck molecular force field (MMFF) followed by considering distance-dependent dielectric constant of 1.0, convergence criterion or root-mean-square (RMS) gradient at 0.01kcal/mol \AA and the iteration limit set to 10,000. The energy-minimized geometry was used for calculation of various 3D descriptors. All molecules were subsequently aligned by an atom based alignment technique using the unsubstituted thiazolidinone derivative 5a (Fig. 1).

3D-Descriptor Calculations

After suitable alignment of the selected molecules, a common rectangular grid (lattice) was generated using the 3D-QSAR module of V Life MDS. The steric, electrostatic and hydrophobic interaction energies were computed at the lattice points of the grid using a methyl probe of charge +1. These interaction energy values were considered for relationship generation and utilized as descriptors. The pre-processing of the independent variables (3D descriptors) was done by removing invariable columns. The QSAR models were obtained by manual data selection type algorithm of training and test set data. The training and test set were selected such that they followed the unicolun statistics, i.e., maximum of the test was less than maximum of training set and minimum of the test set was greater than of training set, which is a prerequisite for further QSAR analysis. This indicated that the test is interpolative i.e., derived from the min-max range of training set.

For the SW- k Nearest Neighbour Molecular Field Analysis (SW-kNN; Model 1), five molecules, namely 5d-5f, 5j, 5l were selected as the test set while the remaining 11

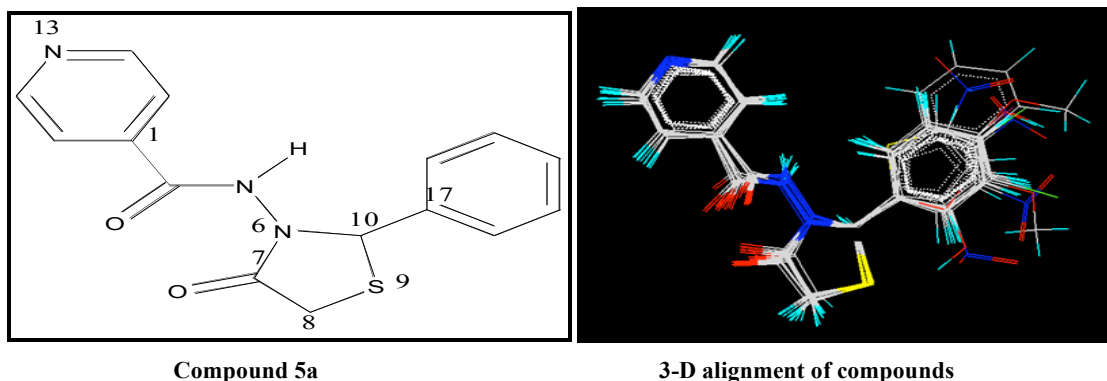


Fig. (1). 3-D alignment of 4-thiazolidinones for QSAR models

molecules (5a-c,g-i,k,m-p) were used as the training set. In the Partial Least Square Linear Regression Analysis (PLRS; Model 2) and Multiple Regression Analysis (MLR, Model 3), compounds 5c, 5d and 5f were used as test set while 5a-b, e, g-p were used as the training test.

Feature Selection and Model Development

An integral aspect of any model-building exercise is the selection of appropriate set of features with low complexity and good predictive accuracy [39]. For all the developed QSAR models, the Stepwise (SW) forward-backward variable selection method was employed to derive the best equations [40]. For the QSAR models, the cross-correlation limit was set at 0.5, number of variables at 4, and the term selection criteria at r^2 for model 1 and q^2 for models 2 and 3 respectively. An F value was specified to evaluate the significance of a variable. The variance cut-off was set at 2, with autoscaling in which the number of random iterations was set at 10. Additionally for the kNN model, the number of maximum to minimum neighbours was set at 5:2. The 3D-descriptors were considered as independent variables and biological activity as dependent variables for the QSAR models.

Statistical Analysis

The SW- kNN MFA, PLSR and MLR methods of analysis were used to derive the 3D QSAR equations. Statistical parameters employed were n number of compounds in regression, the regression coefficient r^2 , r^2_{se} (standard error of squared correlation coefficient), the F-test (Fischer's value) for statistical significance, the cross-validated correlation coefficient q^2 and q^2_{se} (standard error of cross-validated squared correlation coefficient). Regression correlation coefficient values close to 1.0 represent the best fit of the regressions [41]. The predictive ability (q^2) of the generated models was evaluated by cross validation using a 'leave one-out' (LOO) method [42]. The external predictive power $pred_r^2$ of the model was also assessed by predicting $\log IC_{50}$ value of test set molecules, which were not included in the QSAR model development. The QSAR investigations resulted in several 3D QSAR equations, the best three are discussed.

RESULTS AND DISCUSSION

Synthesis

The synthetic strategies adopted to obtain the intermediate and target compounds are illustrated in

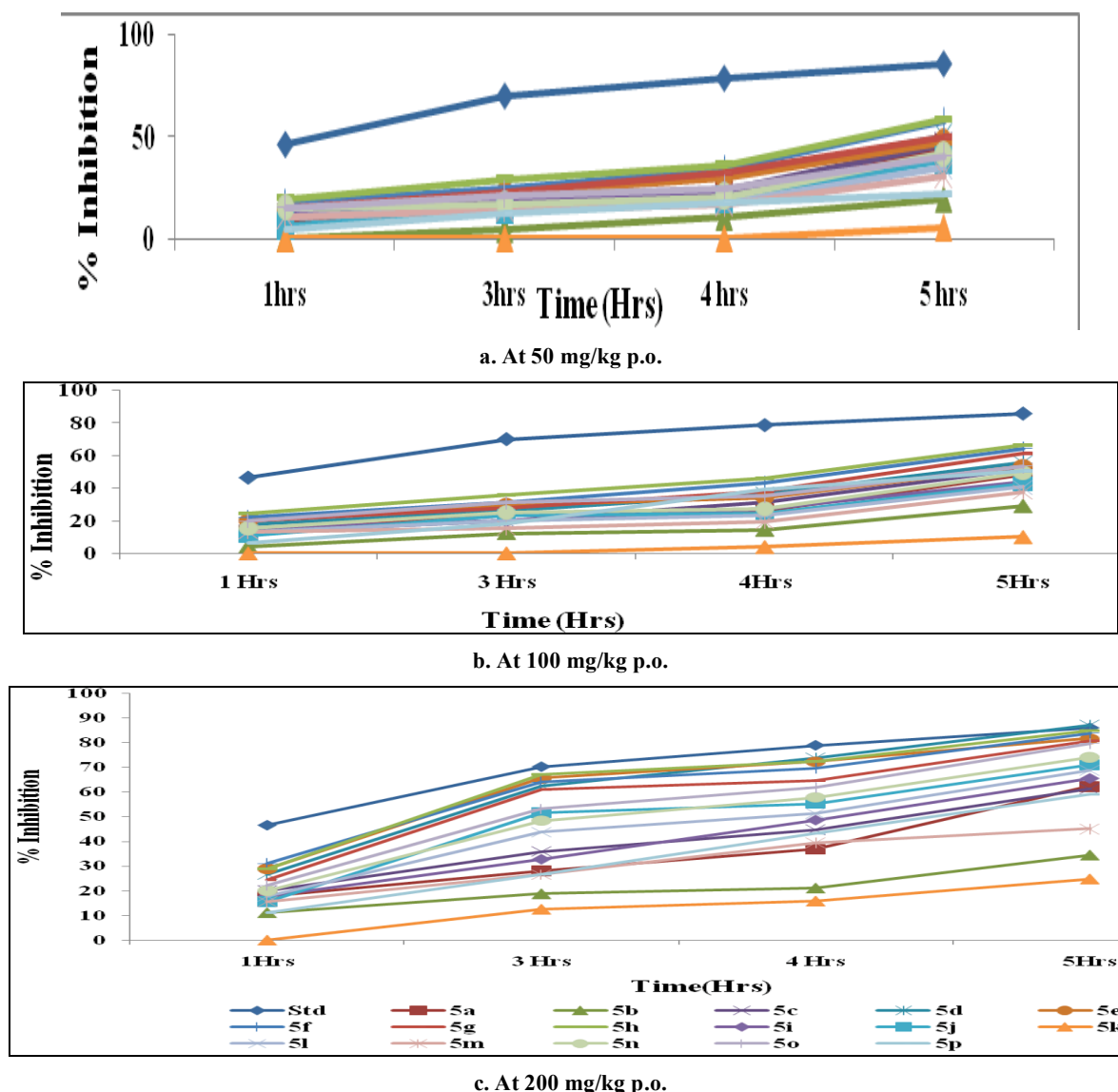
Schemes 1 and 2 respectively. The microwave assisted synthesis of the Schiff's base intermediates (3a-p) involved the reaction of isonicotinyl hydrazone (INH,1) with various substituted aryl/hetero aryl aldehydes (2a-p) in water in shorter reaction times (6-9 mins) with improved yields (86.7-99.2%) as compared to the reported conventional methods. The intermediates were converted into 4-thiazolidinones (5a-p) on ultrasound assisted reaction with mercaptoacetic acid(4) in presence of anhydrous $ZnCl_2$ and molecular sieves in good yields (80.3-96.8%) in reduced reaction times (30-45 min). Satisfactory IR, 1H -NMR and MS characteristics were obtained. The 1H -NMR spectra of 3a-p showed a singlet signal for =CH proton between 7.4-9.48 ppm, confirming formation of Schiff's bases. The 1H -NMR spectra also exhibited a signal between 7.01-8.66 ppm for the N-H proton. The 3J coupling constants of these two protons were almost negligible. However, the theoretical 3D optimisations of compounds 3a-p using ChemDraw Ultra 8.0, V-Life MDS and ACD/ChemSketch indicated that the bulky substituted phenyl and pyridine carboxamide groups are at the same side of the N=C bond, indicating the Z-configuration of Schiff's bases. The Z-configuration will be further confirmed through NOE (Nuclear Overhauser effect) experiments. However, in the 1H -NMR spectra of 3k, the coupling constant of 16 Hz states that the two olefinic protons are located on opposite sides of the C=C bond. In the 1H -NMR spectra of all compounds of series 5, a singlet signal equivalent to 1 proton between 5.22-6.38 ppm (C-2, CH) and a doublet of doublet signal equivalent to 2 protons between 3.36-3.94 ppm; 3.14- 3.85ppm (C-5, CH_2) was observed, considered to be a strong confirmation of ring closure representing the formation of thiazolidinone nucleus. The calculated J value in the range of 8-16 Hz justified the presence of the geminal protons at the C-5 position of the thiazolidinone ring. The elemental analysis results of all compounds were within $\pm 0.4\%$ of the theoretical values.

Biological Investigations

The acute toxicity studies of the synthesized compounds did not produce any morbidity and mortality up to a maximum dose of 2000 mg/kg body weight in mice. The maximum dose of up to 200 mg/kg of test compounds was selected for further biological studies in animal models.

Evaluation of Anti-Inflammatory Activity: Carrageenan Induced Paw Edema Inhibition Model in Rats

The *in vivo* anti-inflammatory activity of synthesized intermediates (3a-p) by carrageenan induced paw edema test



Mean ± SEM of 6 rats. $p < 0.01^{**}$, $p < 0.05^*$ compared with control, ns-non significant; One way ANOVA followed by Dunnett's test.

Fig. (2). Effect of 5a-p on % inhibition of rat paw edema.

in rats showed varying degree of anti-inflammatory activity from 15.05% - 55.91% at 200mg/kg p.o. However, all the synthesized Schiff's bases were less active as compared to standard indomethacin (10 mg/kg p.o., 86.02%, $p < 0.01$).

As compared to the intermediates, the 4-thiazolidinones (5a-p) at graded doses of 25, 50, 100 and 200 mg/kg p. o. exhibited significant anti-inflammatory activity with dose dependency. Among the synthesized 4-thiazolidinones, the introduction of electron withdrawing nitro substituent at para/ortho positions of phenyl ring as in 5f, and 5h, resulted in significant inhibition of edema in comparison to the meta substituted derivative 5g (80.64%, $p < 0.01$).

As these compounds exhibited increasing anti-inflammatory activity in the second phase of carrageenan induced edema, they may exert their activity through inhibition of enzymes which are important in the arachidonic acid cascade, thereby preventing the formation of inflammatory prostaglandins from arachidonic acid. The ulcerogenic liabilities of tested compounds were either

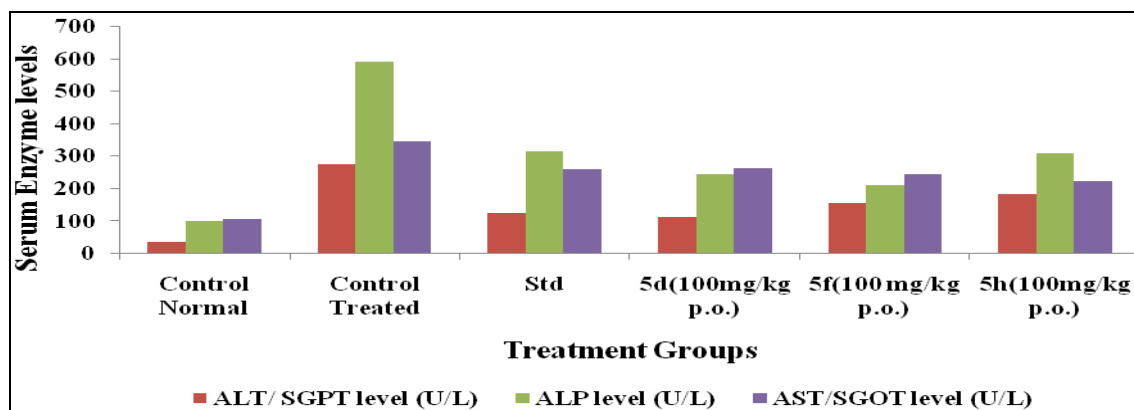
absent or much less than that of indomethacin at all graded doses. The results of the anti-inflammatory screening of the test compounds are summarized in Figs. (2a-c) respectively.

Serum Levels of Marker Enzymes in Carrageenan Induced Paw Edema Model

In the control carrageenan treated group, significant increase in the levels of AST, ALT and ALP in serum were observed. However compounds 5d and 5f, at the dose of 100mg/kg p.o. were effective in lowering the elevated levels of enzymes in serum comparable to standard Indomethacin thereby suggesting their membrane stabilising potential (Fig. 3).

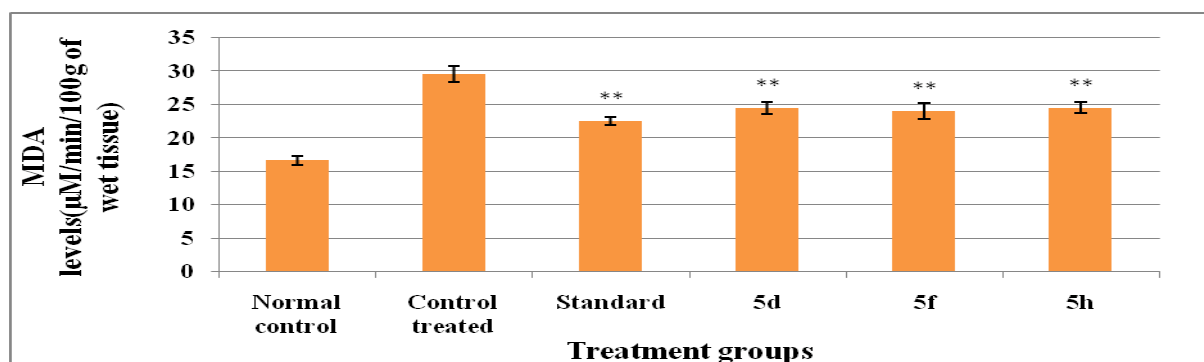
Myeloperoxidase Level in Edematous Tissue in Carrageenan Induced Paw Edema Model

A significant increase in myeloperoxidase activity in edematous tissue in the control carrageenan treated group was observed which was effectively inhibited by the tested 4-thiazolidinones. Compound 5f was found to significantly



ALT: Alanine transaminase; ALP: Alkanine phosphatase; AST: Aspartate transaminase; 5d, f, h: Test thiazolidnones; Mean \pm SEM (n=6); $p < 0.01^{**}$, $p < 0.05^{*}$ compared with control, ns-non significant; One way ANOVA followed by Dunnett's test

Fig. (3). Serum levels of Marker enzymes in the carrageenan induced paw edema model



5d, f, h: Test thiazolidnones; Mean \pm SEM (n=6); $p < 0.01^{**}$, $p < 0.05^{*}$ compared with control, ns-non significant; One way ANOVA followed by Dunnett's test

Fig. (4). Myeloperoxidase level in edematous tissue in carrageenan induced paw edema model

($p < 0.01$) lower elevated levels of MPO in edematous tissue when compared to indomethacin. The inhibition of MPO can be well correlated with the reduction of edema formation (Fig. 4). COX Inhibitory Screening Assay (COX-1/2)

In Vitro COX-1 Inhibition

All compounds inhibited COX-1 in the range of 22.61% to 83.33% when added to the assay mixture at 200 μ M and act as competitive inhibitors. N-[2-(4-nitrophenyl)-4-oxo-1,3-thiazolidin-3-yl] pyridine-4-carboxamide (5f) exhibited the highest inhibitory activity (% inhibition: 89.28%, $p < 0.01$). The ortho/meta substituted nitro derivatives with lower inhibitory activity (64.28%, $p < 0.01$ and 78.57%, $p < 0.01$ respectively) suggests that the addition of the nitro substituent at the para position of the phenyl ring is favourable for activity. Addition of the hydroxyl group at para/ortho position of the phenyl ring as in compounds 5c and 5b resulted in less active compounds [p-OH(36.90%, $p < 0.01$); o-OH(22.61%, $p > 0.05$)] compared to compound 5f. When a methoxy substituent was added to the meta position of the para hydroxyl derivative, the inhibition was significantly improved (71.42%, $p < 0.01$). It was evident from the data, that the addition of methoxy substituent as in 5l and in the p-methoxy derivative 5j (% inhibition: 70.23%, $p < 0.01$) was favourable for activity. Compound 5d with a para chloro substituent on the phenyl ring showed dramatic

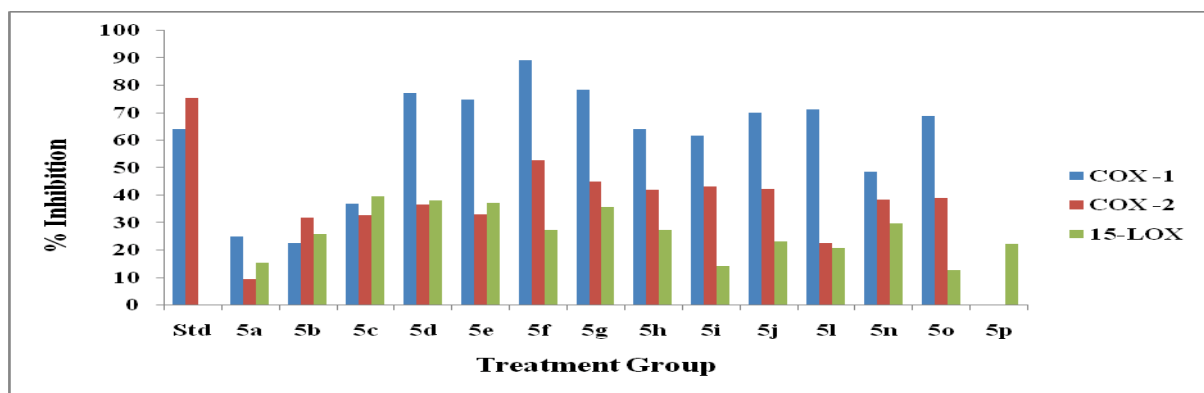
improvement in the inhibitory activity (83.33%, $p < 0.01$) which is comparable to 5f, the most active compound in the series.

In Vitro COX-2 Inhibition

Tested compounds showed low to moderate COX-2 inhibition at 200 μ M acting as competitive inhibitors of the enzyme. Compound 5f exhibited the highest inhibitory activity (52.80%, $p < 0.01$). Substitution of the nitro group at the meta/ortho position resulted in reduction in inhibitory activity [m-nitro(45.20%, $p < 0.01$); o-nitro(42.00%, $p < 0.01$)]. In the halogen series, interestingly the addition of fluoro substituent at the para position of the phenyl ring in 5i exhibited significant improvement in the inhibitory activity (43.20%, $p < 0.01$) as compared to the para/ meta substituted chloro analogues. Standard indomethacin at 200 μ M exhibited 64.28% inhibition of COX-1 and 75.60% inhibition of COX-2.

Soyabean Lipoxigenase Inhibitor Screening Assay

In the 5-LOX inhibitory assay, most compounds showed low to moderate inhibitory activity. The p-hydroxy compound 5c was the most active in the series with % inhibition of 39.80% ($p < 0.01$). In addition the p-chloro (5d) and m-chloro derivatives (5e) also showed moderate LOX inhibitory activity (38.30%, $p < 0.01$ and 37.31%, $p < 0.01$)



5a-j,l,n-p: Test 4-thiazolidinones; Mean \pm SEM (n=3); $p < 0.01^{**}$, $p < 0.05^*$ compared with control, ns- non significant; One way ANOVA followed by Dunnett's test

Fig. (5). Effect of 4-thiazolidinones on *in vitro* COX-1/2 and 15-LOX inhibitory assay.

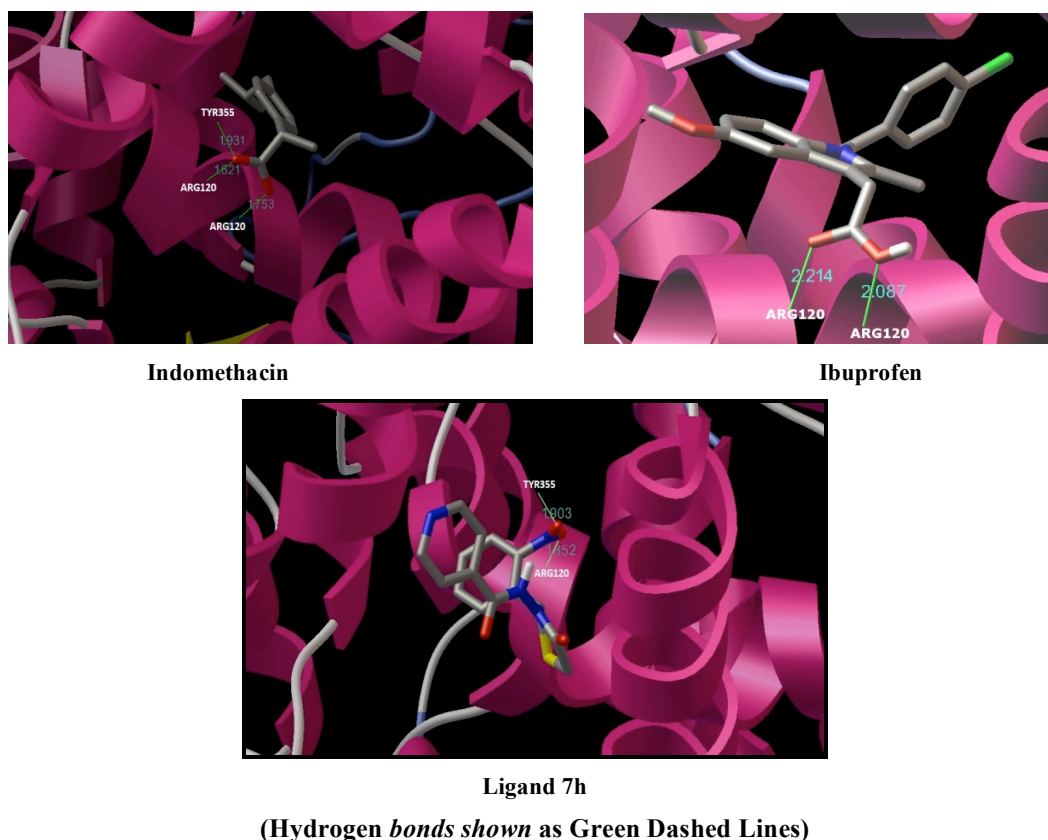


Fig. (6). Binding into active site of COX-1 enzyme.

respectively) suggesting that *p*-hydroxy, *p*-chloro and *m*-chloro groups may be important for significant LOX inhibitory activity (Fig. 5).

Molecular Docking Study

In an attempt to further corroborate the design of new isoniazid analogues, aimed at better COX-1/2 and LOX activity, the binding affinities of the active 4-thiazolidinones were investigated using the advanced docking program AutoDock 4.2. For the COX-1 enzyme, good correlation between experimental (IC_{50}) and predicted *in vivo* anti-inflammatory results were obtained for compounds (r^2 of 0.676). In the COX-1 studies (PDB code: 1EQG), ligands 5f and 5h exhibited binding and docking energies comparable

to standard drugs, Ibuprofen and Indomethacin respectively. The obtained COX-1 complex with Ibuprofen (ΔG_b : -8.39 Kcal/mol; Docking energy: -9.90 Kcal/mol) reveals a binding pose in which the carboxylate group forms three hydrogen bonds; two bonds with Arg120 and one hydrogen bond with Tyr 355 residues present at the mouth of the cyclooxygenase active site which is in good agreement with the crystal structure of COX-1. In addition, hydrophobic residues such as Val349, Met522, Gly526, Ala527, Phe518 and Leu531 surround the phenyl isopropyl group, within van der Waals contact distance. The main interactions observed for standard Indomethacin and COX-1 are two hydrogen bonds involving the carboxylate group with Arg120. Visual inspection of the COX-1 complex with 5h (ΔG_b : -8.14 Kcal/mol; Docking energy: -9.25 Kcal/mol) reveals similar binding orientation as

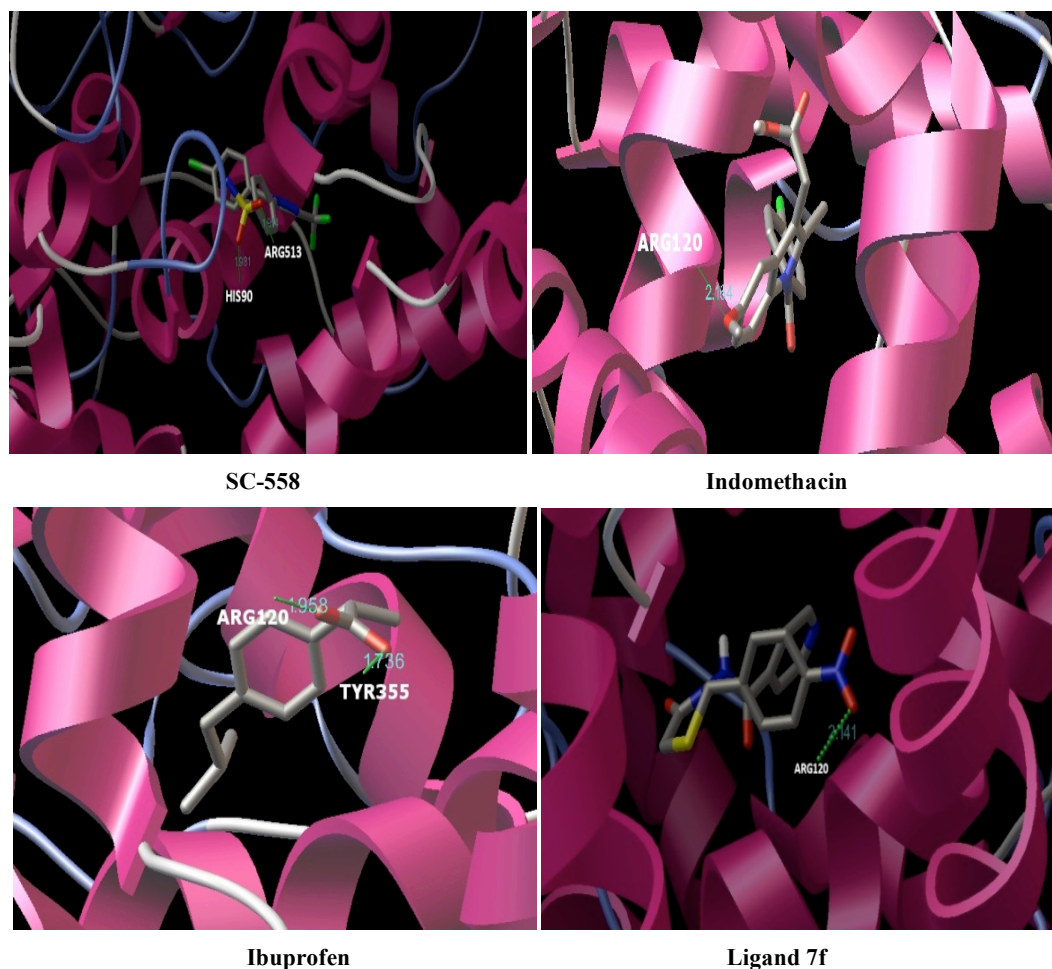


Fig. (7). Binding into active site of COX-2 enzyme.

the complex of Ibuprofen with COX-1, involving hydrogen bonding interactions of one of the oxygen atom of the nitro group with Arg120 and Tyr355 respectively (Fig. 6).

(Hydrogen Bonds Shown as Green Dashed Lines)

From the docking studies of 4-thiazolidinones on 1CX2, it was observed that the computed binding energies showed good correlation with the *in vivo* anti-inflammatory activity (r^2 of 0.642). The co-crystallized ligand SC-558 displayed lowest binding (-10.66 Kcal/mol) and docking energies (-12.63 Kcal/mol) which confirms that it is a selective COX-2 inhibitor. The COX-2 complex with SC-558 reveals a binding pose involving hydrogen bonding interactions of oxygen atoms of the sulfone group at the mouth of the binding channel with His90 and Arg513. The sulfone substituted phenyl ring is surrounded by Phe518, Ile517, Tyr355, Ser353 and Leu352 in hydrophobic contacts. Additional hydrophobic interactions involving Arg120, Tyr385, Trp387, Ala527, Met522 and Leu531 are observed which surround the bromophenyl ring. All the other studied ligands exhibited higher energies as compared to SC-558. Ligands 5d, e, f, h, o exhibited binding and docking energies comparable to standard Indomethacin. The effective fit of these compounds into the COX-2 active site showed good co-relation of the experimental biological activities with their ΔG_b values comparable to standard Indomethacin (Fig. 7).

In the LOX binding studies, ligand 5d exhibited most favourable binding within both the β -barrel and catalytic domain of 1LOX (ΔG_b : -8.20 Kcal/mol, Docking energy: -9.50 Kcal/mol; ΔG_b : -8.22 Kcal/mol, Docking energy: -9.07 Kcal/mol respectively) through hydrogen bond interaction with Cys 97 through the -NH atom of its amide group within the β -barrel domain. Furthermore, hydrophobic residues, such as Met377 and Ser382 surround the chlorophenyl ring within van der Waals contact distance indicating that they may be important for activity. The effective fit of ligands 5d and 5c into the LOX active site showed good correlation of the *in vitro* LOX enzyme activities with their ΔG_b values.

3D-QSAR Study

To elucidate the effect of the aromatic substitutions at the C-2 position of the thiazolidinone ring on the anti-inflammatory activity, their activities were converted into logarithmic values. Using the QSAR module of V-Life MDS, the 3D-QSAR investigations were performed using the SW-kNN, PLRS and MLR models. The training set/test set selections were done manually such that the compounds populate the wide range of anti-inflammatory activities in similar proportions. The validation parameters for the 3D QSAR models are illustrated in Table 1.

The developed QSAR models were found to be statistically significant and predictive in terms of r^2 , q^2 , F and pred_r^2 values. SW-kNN model showed good internal

Table 1. Comparative Data of Validation Parameters for the 3D-QSAR Models

Parameter	Model 1(kNN)	Model 2(PLSR)	Model 3 (MLR)
Contributing descriptor/ Equation	Electrostatic E_545(0.9050- 1.2450)	1) Log IC ₅₀ =-0.0396 E_609 – 0.012 S_697- 0.0107 E_546-0.0068 S_771-0.3499	2) Log IC ₅₀ =-0.0342 E_609 –0.0166S_697- 0.0219E_590- 0.0097 S_771 – 0.2131
Training set(N)	11	11	11
Test set (N)	5(5d-f,5j,5l)	3 (5c,5d , 5f)	3(5c,5d , 5f)
DF	9	8	6
r ²	--	0.9630	0.9856
r ² _se	--	0.0727	0.0524
q ²	0.5568	0.8408	0.8988
q ² _se	0.2500	0.1507	0.1388
pred_r ²	0.7859	0.7393	0.5884
pred_r ² se	0.1918	0.2646	0.3325
F test	--	104.0577	102.5127
Knearest neighbour	2	--	--

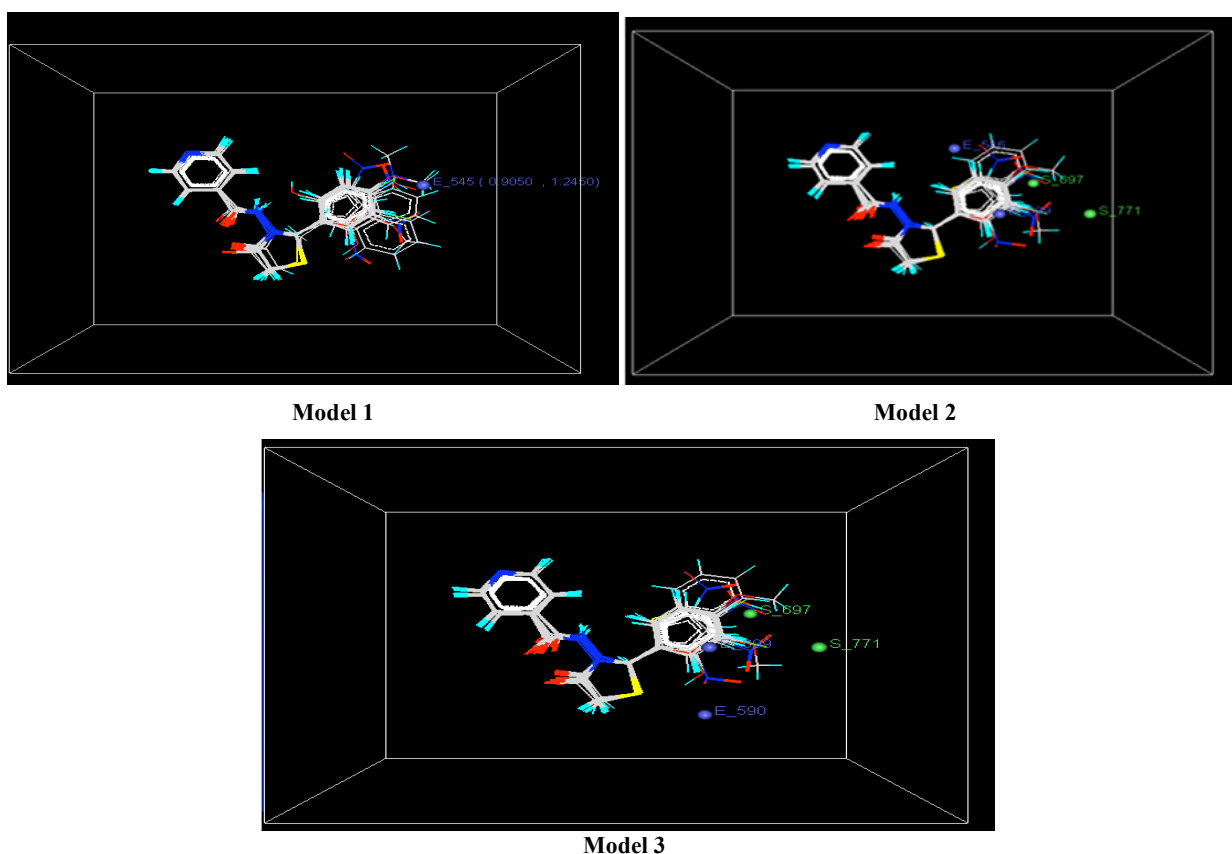


Fig. (8). Relative positions of local fields around 4-thiazolidinones.

predictive ability ($q^2 = 0.5568$) and a good fitness plot with an optimal ability to predict the activities of test set molecules ($\text{pred}_r^2 = 0.7859$) which have not been included to build the QSAR model. Model 2 and 3 also displayed excellent fit ($r^2 = 0.9630, 0.9856$) with good internal predictive abilities ($q^2 = 0.8408, 0.8988$). However, the ability of MLR model to predict the activities of test set

molecules was lower ($\text{pred}_r^2 = 0.5884$ and) as compared to the PLSR model ($\text{pred}_r^2 = 0.7393$).

Interpretation of QSAR Models

The local electrostatic and steric fields around aligned molecules found to be important for anti-inflammatory activity variation by the developed models are shown in Fig. (8).

In model 1, the electrostatic field descriptor E_545 at the para position of C-2 substituted aromatic ring on the thiazolidinone nucleus has positive coefficient in the range of 0.9050 to 1.5130 and was found to contribute significantly for anti-inflammatory activity of the molecules. The nitro (5f-h) and *p*-fluoro substituted (5i) 4-thiazolidinones displayed positive values for the descriptor E_545 within the range as derived from model 1 indicating that the presence of electron withdrawing functional groups like -NO₂, -F at para position are favourable for increase in anti-inflammatory activity.

In models 2 and 3, three electrostatic field descriptors E_609, E_546 and E_590 (blue points) and two steric field descriptors S_697 and S_771 (green points) contribute for the anti-inflammatory activity of the molecules. Descriptors E_609, S_697 and S_771 are common in both models indicating their significance for the anti-inflammatory activity.

In model 2, the negative coefficients for the electrostatic parameters E_609(-50.80%) and E_546(-10.84%) indicate that negative electrostatic potential is favoured for increase in activity and hence more electronegative substituents should be preferred in these regions (meta position of the phenyl ring at C-2 position of the thiazolidinone ring). The steric field descriptors S_697 and S_771 contributed negatively (-27.47% and -10.89% respectively) indicating that less bulky substituents are preferred in these positions (meta and para position of phenyl ring at C-2 position of the thiazolidinone ring) for optimal biological activity. In model 3, the electrostatic parameter E_609 also correlated negatively (-39.70%) with biological activity similar to model 2, suggesting that more electronegative substituents should be preferred in these regions (meta position of the phenyl ring at C-2 position of the thiazolidinone ring). However, electrostatic descriptor E_590 contributed positively (12.08%), indicating that less electronegative groups may be favoured at the ortho position of the phenyl ring at C-2 position of the thiazolidinone ring. The negative coefficients for the steric descriptors S_697(-34.31%) and S_771 (-13.90%) as in model 2, showed that more bulky substituents at the meta and para positions of the phenyl ring at C-2 position of the thiazolidinone ring are detrimental for the anti-inflammatory activity.

The results of the 3D-QSAR analysis of the 4-thiazolidinones by the kNN, PLSR and MLR models evidenced that the substituents similar to electron withdrawing functional groups like -NO₂, -Cl which were found to be favourable for the activity and contributing to the electronic descriptors E_609, E_545 and E_546 and possessing similar + σ and + π values like -Br, -OCF₃, -CF₃, -CF₃SO₂ may be substituted in these regions to increase the activity. Also substituents possessing + σ and - π values like -COOH, CH₃CO-, -CN, -CONH₂, -CH₃SO₂, -SO₂NH₂ can also be substituted to study their effect on the activity. Further, the appearance of steric descriptors in both the PLSR and MLR models indicated that less bulky substituents are favoured at these positions for optimal biological activity.

Among the models studied, the kNN model was found to be the best model with good prediction capabilities while in the studied regression models, the PLSR model was found to be more suitable with significant *r*², *q*² and pred_*r*² values as compared to the MLR model.

MLR and PLSR are the most fundamental and common modelling methods for regression QSAR and are favoured due to their simplicity and ease of interpretations. However, the interpretations by MLR may not be accurate as collinear descriptors have the potential to influence the coefficients such that erroneous values may be assigned as reflected in the lower pred_*r*² as compared to the PLSR model. PLSR model is more appropriate when the number of features greatly exceed the number of samples and when features are highly collinear. Amongst the derived QSAR models, the KNN model is the advanced model that requires practically no training and is asymptotically optimal. However these classification methods are suitable for the prediction of compound class (active vs. nonactive) when the availability of activity information is limited. On the other hand, regression methods are suitable for quantitative (activity values e.g., IC₅₀ or EC₅₀) prediction when sufficient activity information of compounds possessing the same property is available.

CONCLUSIONS

NSAIDs are widely used for treatment of inflammatory disorders. However as their chronic use has shown adverse effects, especially gastric disturbances, attempts have been made to synthesize 4-thiazolidinones as dual COX/LOX inhibitors, preventing the biosynthesis of both prostanoids and leucotrienes, thereby acting as potent anti-inflammatory agents. The anti-inflammatory assay measured by inhibition of carrageenan induced rat paw edema, showed that compounds 5d, 5f and 5h were the most active compounds with low gastric ulcerogenic effects as compared to standard indomethacin. Molecular modelling studies with COX-1/2 and LOX revealed good binding affinities comparable to the known NSAIDs like indomethacin and ibuprofen. 3D-QSAR studies of the synthesized compounds employing kNN, PLSR and MLR models indicated the presence of electron withdrawing functional groups like -NO₂, -Cl contributing significantly for the anti-inflammatory activity. In addition, decrease in steric interactions at certain lattice points could be beneficial for improved potency of the 4-thiazolidinone derivatives. Thus the developed 3D-QSAR models could be useful for predicting activity of structurally similar analogs and could also guide in design of new molecules with improved anti-inflammatory potential with low ulcerogenic activity. Finally as both COX and LOX are up-regulated in various cancers, development of drugs targeting both enzymes would be useful to further design drug for chemoprevention.

CONFLICT OF INTEREST

The authors confirm that this article content has no conflicts of interest.

ACKNOWLEDGEMENTS

The authors wish to thank the Management and Principal, Padm. Dr.D.Y. Patil Institute of Pharmaceutical Sciences and Research, Pune (India) and National Toxicology Centre, Pune (India) for providing the necessary infrastructural facilities to carry out this work. The authors thank SAIF/CIL, Punjab University, Chandigarh (India) for providing the spectroscopic data of compounds. The authors would like to specially mention the contribution of Rasa Life Sciences, Pune (India) for the Molecular Docking studies.

REFERENCES

- [1] Gao, H.M.; Hong, J.S. Why neurodegenerative diseases are progressive: Uncontrolled inflammation drives disease progression. *Trends Immunol.*, **2008**, *29*(8), 357-5.
- [2] Klegeris, A.; McGeer, P.L. Non-Steroidal Anti-Inflammatory Drugs (NSAIDs) and other anti-inflammatory agents in the treatment of neurodegenerative disease. *Curr. Alzheimer Res.*, **2005**, *2*(3), 355-65.
- [3] Rao, P.; Knaus, E.E. Evolution of nonsteroidal anti-inflammatory drugs (NSAIDs): cyclooxygenase (COX) inhibition and beyond. *J. Pharm. Sci.*, **2008**, *11*(2), 81-110.
- [4] Topliss, J.G. Utilization of operational schemes for analog synthesis in drug design. *J. Med. Chem.*, **1972**, *15*(10), 1006-11.
- [5] Bonde, C.G.; Gaikwad, N.J. Synthesis and preliminary evaluation of some pyrazine containing thiazolines and thiazolidinones as antimicrobial agents. *Bioorg. Med. Chem.*, **2004**, *12*(9), 2151-61.
- [6] Verma, A.; Saraf, S.K. Thiazolidinone- A biologically active scaffold. *Eur. J. Med. Chem.*, **2007**, *xx*, 1-9.
- [7] Terzioglu, N.; Gursoy, A. Synthesis and Isolation of new regioisomeric 4-thiazolidinones and their anti-convulsant activity. *Turk. J. Chem.*, **2005**, *29*(3), 247-54.
- [8] Hrib, N.J.; Jurcak, J.G.; Bregna, D.E.; Burgher, K.L.; Hartman, H.B.; Kafka, S.; Kerman, L.L.; Kongsamut, S.; Roehr, J.E.; Szwczak, M.R.; Woods-Kettelberger, A.T.; Corbett, R. Structure-activity relationships of a series of novel (Piperazinylbutyl) thiazolidinone antipsychotic agents related to 3-[4-[4-(6-Fluorobenzo[b]thien-3-yl)-1-piperazinyl]butyl]-2,5,5-trimethyl-4-thiazolidinone Maleate. *J. Med. Chem.*, **1996**, *39*(20), 4044-57.
- [9] Liesen, A.P.; de Aquino, T.M.; Carvalho, C.S.; Lima, V.T.; de Araújo, J.M.; de Lima, J.G.; de Faria, A.R.; de Melo, E.J.T.; Alves, A.J.; Alves, E.W.; Alves, A.Q.; Góes, A.J.S. Synthesis and evaluation of anti-Toxoplasma gondii and antimicrobial activities of thiosemicarbazides, 4-thiazolidinones and 1,3,4-thiadiazoles. *Eur. J. Med. Chem.*, **2010**, *5*(9), 3685-91.
- [10] Pan, B.; Huang, R.; Zheng, L.; Chen, C.; Han, S.; Qu, D.; Zhu, M.; Wei, P. Thiazolidinone derivatives as novel antibiofilm agents: design, synthesis, biological evaluation and structure-activity relationships. *Eur. J. Med. Chem.*, **2011**, *46*(3), 819-24.
- [11] Tomas'ic, T.; Zidar, N.; Mueller-Premru, M.; Kikelj, D.; Mas'ic, L. P Synthesis and antibacterial activity of 5-ylidenethiazolidin-4-ones and 5-benzylidene-4, 6-pyrimidinediones. *Eur. J. Med. Chem.*, **2010**, *45*(4), 1667-72.
- [12] Patel, N.B.; Shaikh, F.M. Synthesis and antimicrobial activity of new 4-thiazolidinone derivatives containing 2-amino-6-methoxybenzothiazole. *Saudi Pharm. J.*, **2010**, *18*(3), 129-36.
- [13] Kouatli, O.; Geronikaki, A.; Zoumpoulakis, P.; Camoutsis, C.; Sokovic, M.; Ciric, A.; Glamoc'lija, J. Novel 4-thiazolidinone derivatives as potential antifungal and antibacterial drugs. *Bioorg. Med. Chem.*, **2010**, *18*(1), 426-32.
- [14] Knutsen, L.J.S.; Hobbs, C.J.; Earnshaw, C.G.; Fiumana, A.; Gilbert, J.; Mellor, S.L.; Radford, F.; Smith, N.J.; Birch, P.J.; Burley, J.R.; Ward, S.D.C.; James, L.F. Synthesis and SAR of novel 2-arylthiazolidinones as selective analgesic N-type calcium channel blockers. *Bioorg. Med. Chem. Lett.*, **2007**, *17*(3), 662-7.
- [15] Murugesan, V.; Prabhakar, Y.S.; Katti, S.B. CoMFA and CoMSIA studies of thiazolidin-4-ones as anti-HIV-1 agents. *J. Mol. Graph. Modell.*, **2009**, *27*(6), 735-43.
- [16] Gududuru, V.; Hurh, E.; Dalton, J.T.; Miller, D.D. Synthesis and antiproliferative activity of 2-aryl-4-oxo-thiazolidin-3-yl-amides for prostate cancer. *Bioorg. Med. Chem. Lett.*, **2004**, *14*(21), 5289-93.
- [17] Taranalli, A.D.; Bhat, A.R.; Srinivas,S.; Saravanan, E. Anti-inflammatory, analgesic and antipyretic activity of certain thiazolidinones. *Indian. J. Pharm Sci.*, **2008**, *70*(2), 159-64.
- [18] Ottana, R.; Mazzon, E.; Dugo, L.; Monforte, F.; Maccari, R.; Sautebin, L.; De Luca, G.; Vigorita, M.G.; Alcaro, S.; Ortuso, F.; Caputi, A. P.; Cuzzocrea, S. Modeling and biological evaluation of 3,3'-(1,2-ethanediyl)bis[2-(4-methoxyphenyl)-thiazolidin-4-one], a new synthetic cyclooxygenase-2 inhibitor. *Eur. J. Pharmacol.*, **2002**, *448*(1), 71-80.
- [19] Vigorita, M.G.; Ottana, R.; Monforte, F.; Maccari, R.; Monforte, M.T.; Trovato, A.; Taviano, M.F. Synthesis and antiinflammatory, analgesic activity of 3,3'-(1,2-Ethanediyl)-bis[2-aryl-4-thiazolidinone] chiral compounds. Part10. *Bioorg. Med. Chem. Lett.*, **2001**, *11*(21), 2791-4.
- [20] Vigorita, M.G.; Ottana, R.; Monforte, F.; Maccari, R.; Monforte, M.T.; Trovato, A.; Taviano, M.F.; Miceli, N.; Luca, G.D.; Alcaro, S.; Ortuso, F. Chiral 3, 3'-(1,2-ethanediyl)-bis[2-(3,4-dimethoxyphenyl)-4-thiazolidinones] with anti-inflammatory activity. Part 11: Evaluation of COX-2 selectivity and modelling. *Bioorg. Med. Chem.*, **2003**, *11*(6), 999-1006.
- [21] Leval, X.; Julémont, F.; Delarge, J.; Pirotte, B.; Dogné, J.M. New trends in dual 5-LOX/COX inhibition. *Curr. Med. Chem.*, **2002**, *9*(9), 941-62.
- [22] Thomas, A.B.; Tupe, P.N.; Badhe, R.V.; Nanda, R.K.; Kothapalli, L.P.; Paradkar, O.D.; Sharma, P.A.; Deshpande, A.D. Green route synthesis of Schiff's bases of isonicotinic acid hydrazide: *Green Chem. Lett. Rev.*, **2009**, *2*, 23-7.
- [23] Thomas, A.B.; Nanda, R.K.; Kothapalli, L.P.; Hamane, S.C. Synthesis and biological evaluation of Schiff's bases and 2-azetidionones of isonicotinyl hydrazone as potential antidepressant and nootropic agents. *Arab. J. Chem.* (In Press).
- [24] Thomas, A.B.; Sharma, P.A.; Nanda, R.K.; Kothapalli, L.P.; Paradkar, O.D.; Deshpande, A.D. Green route synthesis of 4-thiazolidinone analogs of isonicotinic acid hydrazide. *Green Chem. Lett. Rev.*, **2011**, *4*(3), 211-7.
- [25] Organization for economic co-operation and development. Guidance document on acute oral toxicity testing. Environment Directorate: Paris, **2001**.
- [26] Winter, C.A.; Risley, E.A.; Nuss, G.N. Carrageenan induced edema in the hind paw of rat as an assay for anti-inflammatory drugs. *Proc. Soc. Exp. Biol. Med.*, **1962**, *111*(3), 544-7.
- [27] Kind, P.R.N.; King E.J. Measurements of serum alkaline phosphatase. *Enz. Microb. Technol.*, **1954**, *7*(4), 322-6.
- [28] Davidson, D.F. Measurement of serum alkaline phosphatase. *Enz Microb. Technol.*, **1979**, *1*(1), 9-14.
- [29] Mullane, K.M.; Westlin, W.; Kraemer, R. Activated neutrophils release mediators that may contribute to myocardial injury and dysfunction associated with ischemia and reperfusion. *Ann. NY. Acad. Sci.*, **1988**, *524*, 103-21.
- [30] Graff, G.; Gamache, D.A.; Bradt, M.T.; Spellman, J. M.; Yanni, J.M. Improved myeloperoxidase assay for quantitation of neutrophil influx in a rat model of endotoxin-induced uveitis. *J. Pharmacol. Toxicol. Methods*, **1998**, *39*(3), 169-78.
- [31] Barf, T.; Vallgård, J.; Emond, R.; Häggström, C.; Kurz, G.; Nygren, A.; Larwood, V.; Mosialou, E.; Axelsson, K.; Olsson, R.; Engblom, L.; Edling, N.; Rönquist-Nii, Y.; Ohman, B.; Alberts, P.; Abrahmsén, L. Arylsulfonamidothiazoles as a new class of potential antidiabetic drugs: discovery of potent and selective inhibitors of the 11beta-hydroxysteroid dehydrogenase type 1. *J. Med. Chem.*, **2002**, *45*(18), 3813-5.
- [32] Kulmacz, R.J.; Lands, W.E.M. Requirements for hydroperoxide by the cyclooxygenase and peroxidase activities of prostaglandin H synthase. *Prostaglandins*, **1983**, *25*(4), 531-40.
- [33] Gaffney, B.J. Lipoxigenases: structural principles and spectroscopy. *Annu. Rev. Biophys. Biomol. Struct.*, **1996**, *25*(4), 431-59.
- [34] Available at: <http://www.rcsb.org/pdb/home>
- [35] Available at: <http://www.ebi.ac.uk/thorntonsrv/database/pdbsum/>
- [36] Morris, G.M.; Goodsell, D.S.; Halliday, R.S.; Huey, R.; Hart, W.E.; Belew, R.K.; Olson, A.J. Automated docking using a Lamarckian genetic algorithm and empirical binding free energy function. *J. Comput. Chem.*, **1998**, *19*(14), 1639-62.
- [37] Spoel, D.V.D.; Hess, B. GROMACS-the road ahead: Software Focus. *WIREs Comput. Mol. Sci.*, **2011**, *1*(5), 710-5.
- [38] V Life Sciences Technologies Pvt. Ltd, Pune, Maharashtra, India (Available at: www.Vlifesciences.com)

- [39] Guyon, A.; Elisseeff, A. An introduction to variable and feature selection. *JMLR*, **2003**, *3*, 1157-82.
- [40] Darlington, R.B. *Regression and Linear Models*, McGraw-Hill: New York, **1990**.
- [41] Golbraikh, A.; Tropsha, A. Beware of q². *J. Mol. Graph Model.*, **2002**, *20*(4), 269-76.
- [42] Cramer, R.D.; Patterson, D.E.; Bunce, J.D. Comparative molecular field analysis (CoMFA): effect of shape on binding of steroids to carrier proteins. *Am. Chem. Soc.*, **1988**, *110* (18), 5959-67.

Received: September 24, 2013

Revised: October 12, 2013

Accepted: November 04, 2013

© Thomas *et al.*; Licensee *Bentham Open*.

This is an open access article licensed under the terms of the Creative Commons Attribution Non-Commercial License (<http://creativecommons.org/licenses/by-nc/3.0/>), which permits unrestricted, non-commercial use, distribution and reproduction in any medium, provided the work is properly cited.